IOPscience iopscience.iop.org

Home Search Collections Journals About Contact us My IOPscience

Epitaxial lateral overgrowth techniques used in group III nitride epitaxy

This article has been downloaded from IOPscience. Please scroll down to see the full text article.

2001 J. Phys.: Condens. Matter 13 6961

(http://iopscience.iop.org/0953-8984/13/32/306)

View the table of contents for this issue, or go to the journal homepage for more

Download details:
IP Address: 171.66.16.226
The article was downloaded on 16/05/2010 at 14:04

Please note that terms and conditions apply.

INSTITUTE OF PHYSICS PUBLISHING JOURNAL OF PHYSICS: CONDENSED MATTER

J. Phys.: Condens. Matter **13** (2001) 6961–6975 PII: S0953-8984(01)25168-6

Epitaxial lateral overgrowth techniques used in group III nitride epitaxy

Kazumasa Hiramatsu

Department of Electrical and Electronic Engineering, Mie University, 1515 Kamihama, Tsu, Mie 514-8507, Japan

E-mail: hiramatu@elec.mie-u.ac.jp

Received 24 May 2001
Published 26 July 2001
Online at stacks.iop.org/JPhysCM/13/6961

Abstract
Selective area growth (SAG) and epitaxial lateral overgrowth (ELO) techniques used in group III nitride epitaxy are reviewed. Structurally controlled GaN in line patterns and dot patterns was obtained by using the SAG technique. This structural control technique has been applied to field emitters, waveguides, facet lasers and low-dimensional quantum structures. The ELO technique was originally proposed as a way to reduce dislocation density in epitaxial GaN layers and various ELO techniques have been developed recently. For example, facet-controlled ELO (FACELO) is one of the attractive techniques available for reducing dislocation density. The dislocation density is dramatically reduced to of the order of 10^{5-6} cm^{-2} with good reproducibility. In this article, SAG and ELO techniques related to nitride epitaxy and applications to optical and electronic devices are reviewed. Production of GaN hexagonal pyramids on dot-patterned GaN/sapphire substrates and the FACELO technique are also described as examples of the SAG and ELO techniques.

1. Introduction

Selective area growth (SAG) of III–V nitrides is a promising technique whose value has been demonstrated in the fabrication of cold-cathode emitter tips, low-loss optical waveguides, microprism laser diodes and semiconductor microstructures such as quantum wires and dots. Epitaxial lateral overgrowth (ELO), based on SAG, has recently attracted considerable attention, since ELO is a useful technique for obtaining epitaxial layers with low dislocation density on heteroepitaxial systems. A remarkable reduction in threading dislocation density has been realized in GaN heteroepitaxy on sapphire substrates. A laser diode (LD) fabricated on an epitaxially laterally overgrown GaN (ELOG) substrate has shown a much longer lifetime. SAG and ELO for GaN on sapphire substrates have been demonstrated both in metallo-organic vapour-phase epitaxy (MOVPE) and hydride vapour-phase epitaxy (HVPE).

 © 2001 IOP Publishing Ltd Printed in the UK

In this article, the various SAG and ELO techniques related to nitride epitaxy and their applications are reviewed. Furthermore, the production of GaN hexagonal pyramids on dot-patterned GaN/sapphire substrates and facet-controlled ELO (FACELO) are described as examples of the SAG and ELO techniques.

2. Selective area growth

2.1. Growth and characterization

Wurtzite GaN was obtained in line patterns [1] and dot patterns [2] by using the SAG technique. This structural control technique has been applied to field emitters [3, 4], waveguides [5], facet lasers [6] and low-dimensional quantum structures [7]. Selective area growth of line-patterned GaN and AlGaN by MOVPE was carried out at atmospheric pressure for the first time on MOVPE-grown GaN(0001)/sapphire substrates using SiO_2 masks [1]. It was shown that the selectivity of GaN epitaxy was good; however, that of AlGaN was relatively poor. Ridge growth occurred in the GaN selective-area growth on a linear window wider than 50 μm, but did not occur in the AlGaN selective-area growth. A GaN structure with a triangular cross-sectional shape comprising $\{1\bar{1}01\}$ facets formed on 10 μm wide linear windows in the $\langle 11\bar{2}0\rangle$ direction, as shown in figure 1, which suggests that the $\{1\bar{1}01\}$ facets are the energetically

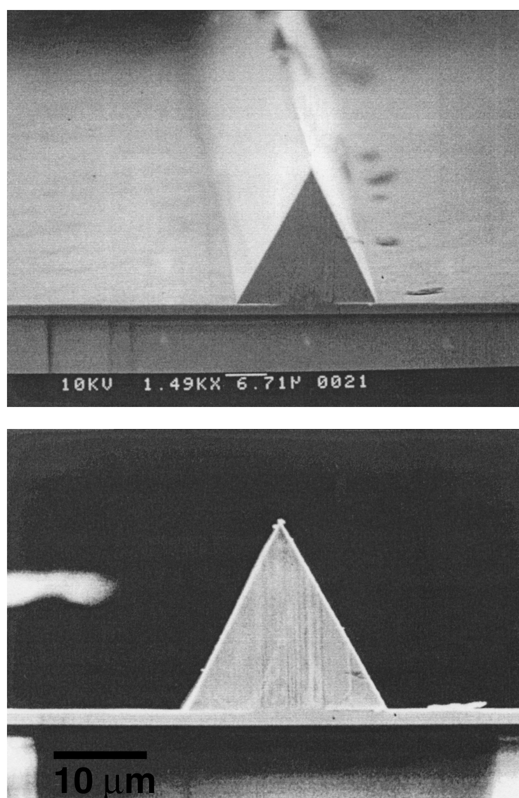

Figure 1. SEM images of GaN grown for 10 min on a 10 mm wide window in the $\langle 11\bar{2}0\rangle$ direction [1].

stable surfaces rather than the (0001) facet. The selective-area growth of GaN was pursued by a few groups, on GaN/sapphire at atmospheric pressure [8] and on GaN/6H-SiC at 45 Torr [3]; no distinct difference was found between the two sets of results. The growth rates (both vertical and lateral), side walls of stripes and roughnesses of side-wall surfaces were dependent on the stripe orientation [9].

Kitamura *et al* [2, 10] fabricated GaN hexagonal pyramids on dot-patterned GaN/sapphire substrates with a 5 μm diameter and a 10 μm space as shown in figure 2 [2].

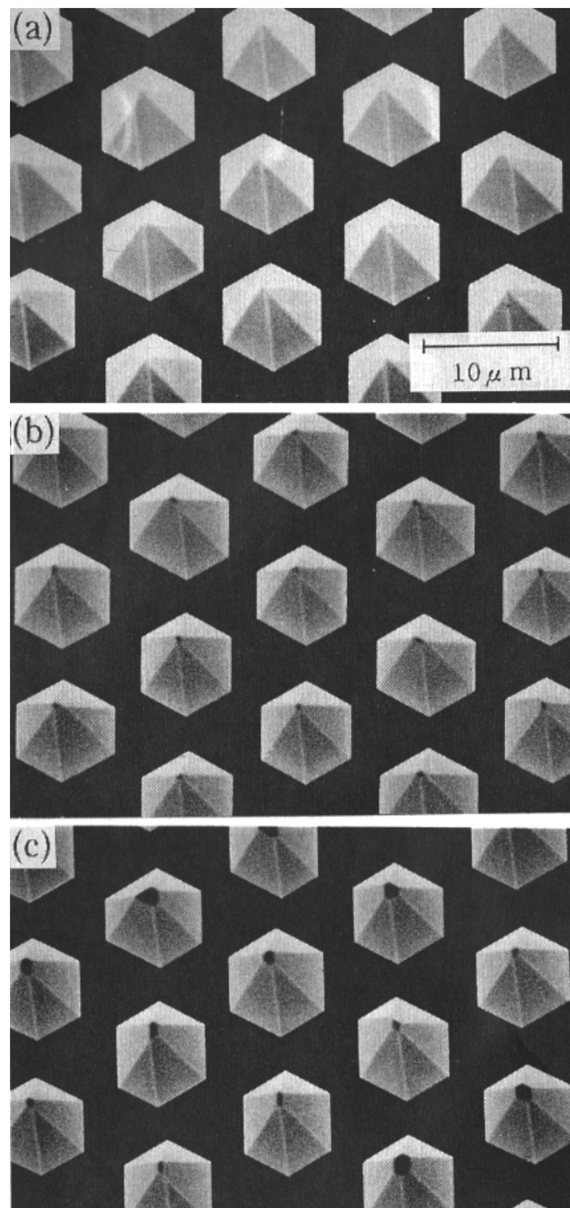

Figure 2. SEM images of MOVPE-grown GaN hexagonal pyramids on a SiO_2 mask patterned on GaN/LT AlN buffer/sapphire at the growth temperatures of (a) 1010, (b) 1025 and (c) 1050 °C [2].

Each structure comprises a hexagonal pyramid covered with six $\{1\bar{1}01\}$ facets. A self-limited (0001) facet sometimes appeared on the top, depending on the growth conditions such as the deposition temperatures and TMG flow rates. The (0001) facet increased in size with increasing growth temperature or with decreasing TMG flow rate. The appearance of the (0001) facet may be determined by the diffusion length of the Ga atom on the (0001) facet. At high growth temperature or small TMG flow rate the diffusion length becomes long, resulting in the appearance of self-limited (0001) facets on the pyramid tops. The fabrication of the hexagonal pyramids was duplicated by a few groups, on dot-patterned GaN/sapphire [11, 12] and GaN/6H-SiC substrates [3]. The incorporation of impurities into GaN during ELO can drastically change the expansion of flat-top (0001) facets [13]. For example, doping of Mg into GaN can greatly increase the vertical-to-lateral growth rate ratio and cause the formation of a large-area (0001) plane.

In addition to SAG using sapphire and 6H-SiC substrates, that using Si substrates is also studied. From the applications point of view, use of Si as the substrate is more attractive, because Si can be a good conductor and is suited to highly sophisticated lithographic techniques. Kawaguchi *et al* fabricated hexagonal pyramid structures on Si(111) substrates using an AlGaN intermediate layer [14, 15]. Figure 3 shows SEM images of the SAG of GaN on a Si substrate with an AlGaN intermediate layer [14]. Uniform pyramid structures are obtained by optimizing the growth temperature and growth time for the AlGaN intermediate layer.

In addition, sub-micron GaN dot and line structures having smaller sizes were fabricated on GaN/sapphire substrates with lined or dotted SiO_2 masks [16]. The patterning of the

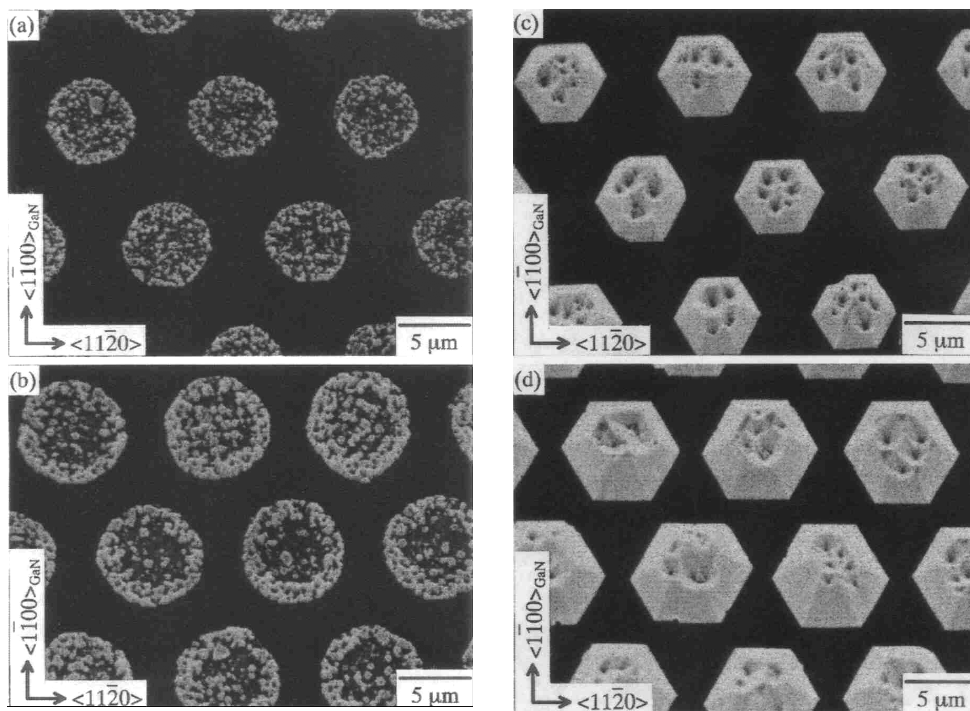

Figure 3. Surface SEM images of the SAG of a GaN patterned micron dot on a Si substrate with an AlGaN intermediate layer for different times of growth of GaN: (a) 0 min, (b) 2 min, (c) 9 min and (d) 19 min [14].

mask was aligned with periods of less than 1.0 μm by using laser holography (He–Cd laser; 422 nm). The relation between the 3D structures of GaN and the growth conditions, such as the growth temperature and V/III ratio, was investigated and GaN hexagonal microprisms (HMPs) with smooth vertical $\{1\bar{1}01\}$ facets were fabricated at growth temperatures higher than 1040 °C [6, 17]. GaN/InGaN/GaN hexagonal pyramids were fabricated and PL spectra of the pyramids were taken [18]. Furthermore, the distributions of defects and strain in the GaN pyramids produced by selective-area growth were clarified by spatially resolved low-temperature luminescence and Raman experiments [19]. Furthermore, InGaN/GaN nano-structures were fabricated by the SAG technique. Arakawa and co-workers fabricated high-density InGaN on hexagonal pyramids of GaN on a substrate patterned by electron-beam lithography [20]. The square openings had side lengths as small as 300 nm. Uniform hexagonal pyramids were realized even when a small pattern was produced. Sakai and co-workers fabricated InGaN quantum dots using selective-area growth on GaN/sapphire substrates with patterned Si masks [7].

2.2. Device applications

Because of the negative electron affinity of AlN and AlGaN and the low positive electron affinity of GaN, these materials are promising for use as cold-cathode emitters. Field emission from GaN hexagonal pyramids on GaN/sapphire [11] and on GaN/6H-SiC [3] has been reported.

Selective-area growth of GaN layers was investigated for low-loss optical waveguide structures of active and passive photonic devices. Layers with a rectangular cross-sectional shape comprising (0001) and $\{1\bar{1}00\}$ facets were fabricated and stimulated emission from the optical waveguides observed at 77 K by photopumping [5]. In addition, GaN HMPs 50 μm in diameter were fabricated [6, 17] and stimulated emission was observed at room temperature using photopumping [17]. The longitudinal modes having a 0.33 nm separation indicate an inscribed hexagonal optical path in the GaN HMP.

3. Epitaxial lateral overgrowth

3.1. Review of ELO techniques

The basic idea of ELO was proposed by Nishinaga *et al* for LPE growth of GaAs on GaAs substrate [21] and GaAs on Si substrate [22]. The lateral epitaxial overgrowth extends over the SiO_2 mask through the opening. Thus dislocations in the substrate under the SiO_2 mask cannot propagate into the lateral epitaxial layer. As regards GaN growth, Usui *et al* [23] and Nam *et al* [24] (see figure 4(a)) applied the ELO technique to GaN and achieved a low dislocation density of the order of 10^7 cm^{-2}. Usui *et al* developed the FIELO (facet-initiated ELO) technique [23], as shown in figure 4(b), using HVPE. Facet structures were formed during the initial stage of the growth. Furthermore, the cross-sectional transmission electron microscope (TEM) image of FIELO GaN [25] shows that facet formation plays a role in changing the propagation direction of the dislocations. The lateral propagation of the dislocations caused by the facet contributes to the reduction of the dislocation density.

In addition to the FIELO technique, several other ELO techniques, such as PENDEO epitaxy [26] (see figure 4(c)), utilization of other masks such as tungsten ones [27, 28] (see figure 4(d)), air-bridged ELO [29, 30] (see figure 4(e)), production of grooved stripe structure [31] (see figure 4(f)) and direct lateral epitaxy [32] (see figure 4(g)), have been proposed. Recently, it was found that two-step ELO growth of GaN is a useful technique for improving the crystalline quality of the ELO GaN through facet control [33, 34]. Hereafter, we call

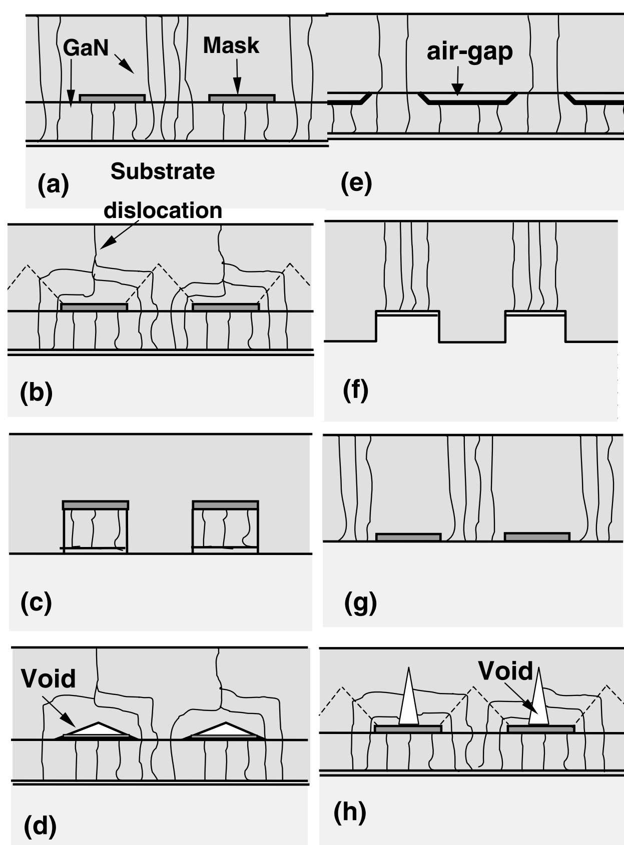

Figure 4. Schematic diagrams of various ELO techniques: (a) the basic ELO idea, (b) FIELO, (c) PENDEO epitaxy, (d) utilization of other masks such as tungsten, (e) air-bridged ELO, (f) production of grooved stripe structure and (g) direct lateral epitaxy.

this technique FACELO (facet-controlled ELO) (see figure 4(h)). It is based on the control of GaN structures by changing the growth conditions during the ELO process. The GaN structures produced using SAG and/or ELO have been controlled by mask size [1], mask direction [1, 9, 24, 35, 36], mask material [27, 28], mask fill factor [37], growth temperature [2, 38–40], reactor pressure [40], flow rate of source [2, 6, 35, 38, 39], ambient gas [41, 42], impurity [43] and substrate [35, 44, 45].

3.2. Experimental production of ELO GaN via a low-pressure MOVPE system and characterization of the dislocation density

The ELO of GaN was achieved via a LP-MOVPE system using a horizontal reactor, on a 4.0 μm thick (0001) GaN layer, which had been prepared on a (0001) sapphire substrate with a low-temperature GaN buffer layer. After the deposition of a SiO_2 film (80 nm thick) by RF sputtering on the underlying GaN, dot patterns or stripe patterns were fabricated by a conventional photolithographic method. TMG (trimethylgallium) and NH_3 were used as the source gases, and H_2 was used as the carrier gas. The growth temperature and the reactor pressure were varied from 925 to 1050 °C and from 40 to 500 Torr, respectively.

The distribution and density of the threading dislocations are characterized by the growth pit density (GPD) method [46, 47], which is performed by growing an InGaN thin layer about 100 nm thick on the GaN epilayer. This is a very convenient technique for characterizing the threading dislocations, because the appearance of the growth pits corresponds to both the mixed and pure edge dislocations with Burgers vectors of $\boldsymbol{a}+\boldsymbol{c}$ and $\boldsymbol{a}$, respectively [48]. Since only a few pure screw dislocations with a Burgers vector of $\boldsymbol{c}$ exist in the layer [25], we neglect the effect of the pure screw dislocations.

3.3. Structures of GaN facet

Figure 5 shows SEM images of cross-sectional shapes of ELO GaN, for different values of P and T, on the SiO_2 stripe along the $\langle 1\bar{1}00\rangle$ directions [32, 40]. The shapes of the ELO GaN are divided into four regions. In region I ($T < 925$ °C), the morphologies are poor; there are large pits on the top and inclined $\{1\bar{1}01\}$ surfaces. In region II, the side walls are composed of the $\{11\bar{2}2\}$ surfaces like in region I, while the (0001) surface becomes smooth. In region III, by decreasing P or by increasing T from region II, the side walls are varied from the inclined $\{11\bar{2}2\}$ surfaces to the vertical $\{11\bar{2}0\}$ surfaces. In region IV, at lower P or higher T, the (0001) surface becomes rough. Consequently, it is found that the effects of decreasing P are similar to those of increasing T in the regions II–IV.

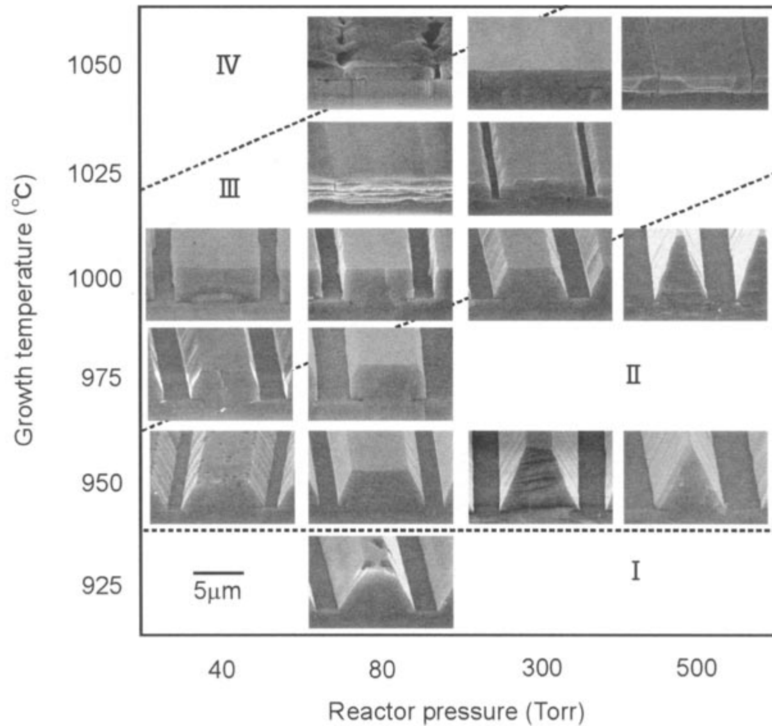

Figure 5. Morphological changes in ELO GaN on the $\langle 1\bar{1}00\rangle$ stripe for different reactor pressures and growth temperatures. The growth time was 30 min [32, 40].

The morphological changes from regions I to IV in ELO are explained as follows. In region I, the (0001) surface degrades because it is not easy for layer-by-layer growth to occur at low T owing to poor surface migration of Ga atoms on the (0001) surface. With increasing

T, however, the surface migration is enhanced and hence the (0001) surface becomes smooth, resulting in region II. In contrast, in region IV, with even lower P or higher T, the surface becomes rough because of the increasing rate of evaporation of absorbed source molecules on the (0001) surface.

This explanation is related to the stability of each surface, which depends mainly on the 'surface energy' and 'stability of surface atoms'. In order to consider these factors, we evaluate just the density of dangling bonds per unit area (DB) and the surface polarity, for simplicity. Figure 6 shows the morphological change from regions II to IV and the corresponding atomic configuration with D_B and the surface polarity for each facet [32]. The change of the morphology with decreasing P is similar to that with increasing T in the regions II–IV. In region II, at high P or low T, the (0001) surface becomes narrow and the $\{11\bar{2}2\}$ surfaces of the sides become broad. In region III at lower P or higher T, $\{11\bar{2}0\}$ surfaces appear instead of $\{11\bar{2}2\}$ ones in the side walls. The morphological change from $\{11\bar{2}2\}$ to $\{11\bar{2}0\}$ should be considered in terms of the stability of each surface which depends mainly on the

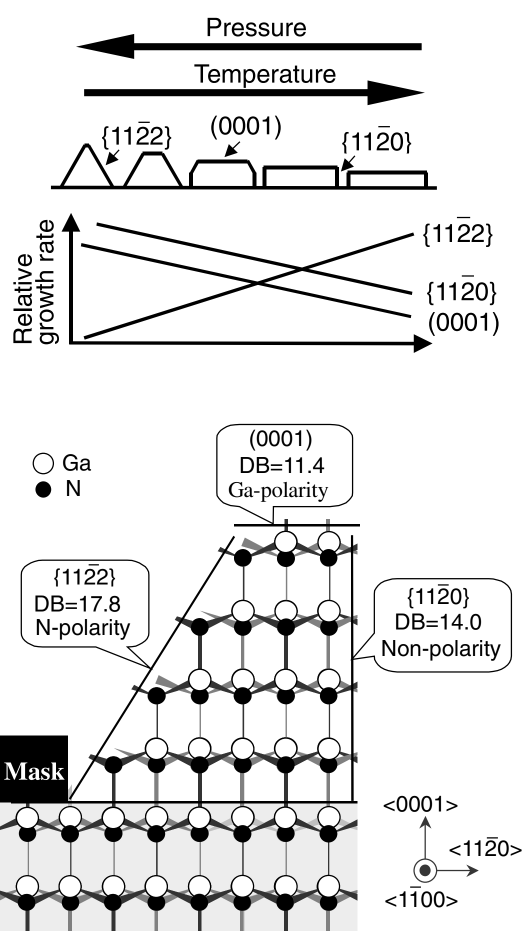

Figure 6. A model of the morphological change in ELO GaN on the $\langle 1\bar{1}00\rangle$ stripe for different reactor pressures and growth temperatures, and the corresponding atomic configuration. Here, 'DB' stands for the density of dangling bonds [32].

'surface energy' and 'stability of surface atoms'. The $\{11\bar{2}2\}$ facet has two possible polarities: N polarity or Ga polarity, on the surface. The surface with N polarity tends to appear because surface nitrogen atoms are stabilized under growth conditions with high V/III source gas ratios like in MOVPE, especially at high P or low T. Therefore, the atomic configuration of the $\{11\bar{2}2\}$ surface with N polarity is dominant, as shown in figure 6. Thus, it is suggested that with increasing T or decreasing P in region II, the growth rate of the $\{11\bar{2}2\}$ surface becomes slow, resulting in narrowing of the $\{11\bar{2}2\}$ surface and broadening of the (0001) surface.

In contrast, in region III, $\{11\bar{2}2\}$ becomes unstable at low P or high T because the surface nitrogen atoms are not stabilized, so the surface becomes narrow. Then the surfaces are $\{11\bar{2}0\}$ and (0001), which are energetically very favourable because the values of D_B for (0001) and $\{11\bar{2}0\}$ (11.4 and 14.0 nm^{-2}) are smaller than that for $\{11\bar{2}2\}$ (17.8 nm^{-2}).

3.4. *Facet-controlled epitaxial lateral overgrowth (FACELO)*

It is possible to control the propagation of threading dislocations on the basis of the change in the facet structure of GaN with the growth conditions. The inclined facet structure and/or the stress due to facet formation cause bending of the mixed and pure edge dislocations with Burgers vectors of $\boldsymbol{a} + \boldsymbol{c}$ and $\boldsymbol{a}$, respectively, and hence the facet has the effect of bending the direction of the threading dislocation and reducing the density [25]. Usui *et al* successfully reduced the dislocation density of the HVPE-grown, thick GaN layer by using inclined facets formed spontaneously during an ELO process [23]. They called this technique FIELO (facet-initiated ELO). The proposed technique employs a facet generated artificially by controlling the growth conditions of ELO, and thus we call this technique FACELO (facet-controlled ELO).

The typical growth process in FACELO is as follows. The first-step ELO has inclined facets of $\{11\bar{2}2\}$, and then in the second-step ELO the lateral growth rate is also increased by changing the growth conditions, and consequently the SiO_2 mask is buried easily. In this case, since the fronts of the dislocations terminate on the inclined $\{11\bar{2}2\}$ facet, the threading dislocations bend towards the mask area during the ELO process. Therefore, some dislocations may disappear in the coalescence region because of the interaction between the dislocations and others coming up to the surface. In this way, the dislocation density on the window area is reduced. This technique is similar to FIELO. However, thickness less than several tenths of a micrometre is needed for the FIELO GaN layer to undergo a reduction of dislocation density, but several micrometres is low enough for the FACELO GaN layer.

Figure 7 shows SEM images of the GaN layer grown by FACELO [49]. In order to observe the threading dislocations, a thin InGaN layer was also grown on the FACELO GaN. The dislocations are observed only in a straight line in the centre of the mask area, which is attributed to the coalescence of ELO. The dislocation density is dramatically reduced over wide areas on both the mask and window areas. The mechanism of the reduction in the dislocation density is discussed in the next section.

3.5. *Characterization of FACELO GaN*

The fine surface structure of the FACELO GaN layer is observed by means of AFM (atomic force microscopy) [49] and TEM [50]. Figure 8(a) shows an AFM surface image of the InGaN epilayer grown on the FACELO GaN layer; this is the same sample as for figure 7 [49]. For comparison, an AFM surface image for an ordinary GaN layer grown on a sapphire substrate using a GaN low-temperature buffer layer is shown in figure 8(b). Pits are clearly observed, corresponding to threading dislocations. From figure 8(b), the estimated dislocation density for the ordinary GaN layer is 5.8×10^8 cm^{-2}. On the other hand, the dislocations exist only

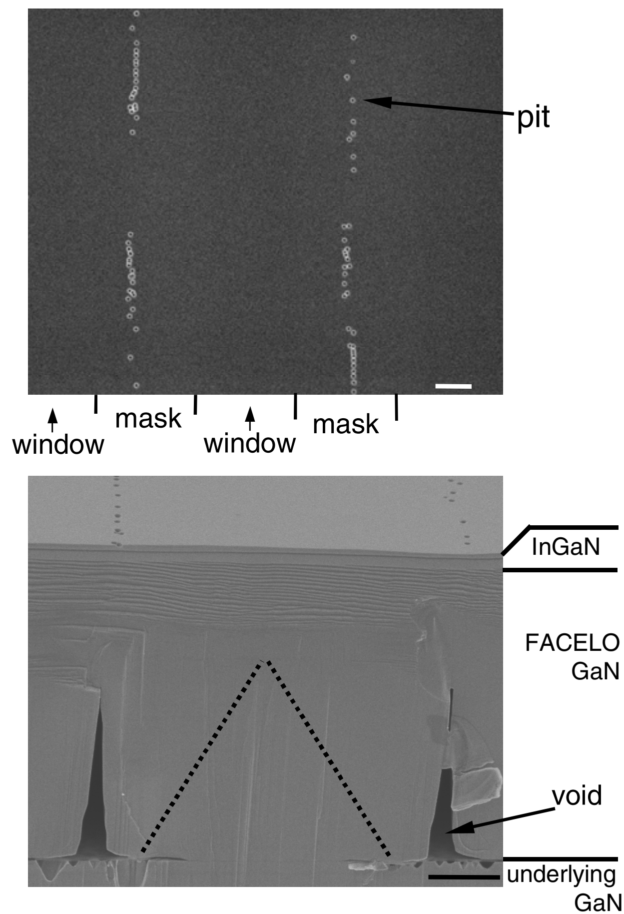

Figure 7. SEM images of FACELO. The dotted line shows the facet structure just after the first-step ELO. The bar indicates 2 μm [49].

in a straight line in the centre of the mask area and there are almost no dislocations over the wide area. The estimated density is of the order of 10^6 cm^{-2}, depending on the position of the surface. To clarify the relationship between bending directions and the character of dislocations, the Burgers vectors of the dislocations are investigated [50]. Figure 9(a) is a bright-field image of FACELO GaN near the mask edge. Figures 9(b) and 9(c) are dark-field images taken at the same position as the bright-field image, with different spots of $(11\bar{2}0)$ and (0002), respectively. The dislocations bent toward the mask areas are visible in both figures 9(b) and 9(c). On the other hand, the dislocations bent parallel to the direction of the mask stripe are invisible in figure 9(c) but they are clearly visible in figure 9(b). From this invisibility, it was found that there are two types of dislocations. Mixed-type dislocations with a Burgers vector of $\boldsymbol{a} + \boldsymbol{c}$ were bent toward the mask areas and terminated by voids. The other type was pure edge dislocations with a Burgers vector $\boldsymbol{a}$, which were bent parallel to the mask stripe. Similar results were observed for HVPE-grown GaN by Sakai *et al* [25].

Figure 10 shows AFM surface images of the as-grown FACELO GaN layer without InGaN together with the as-grown ordinal GaN layer [49]. Monomolecular steps of height 0.25 nm are seen in both AFM images. The steps of the ordinal GaN surface are irregular owing to

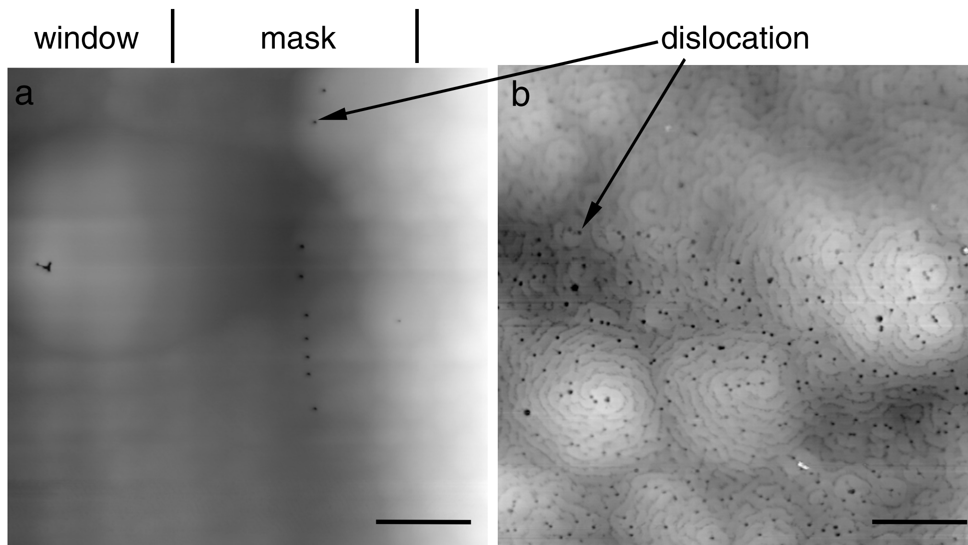

Figure 8. AFM images of (a) InGaN/FACELO GaN and (b) InGaN/ordinary GaN. The bar indicates 2 μm [49].

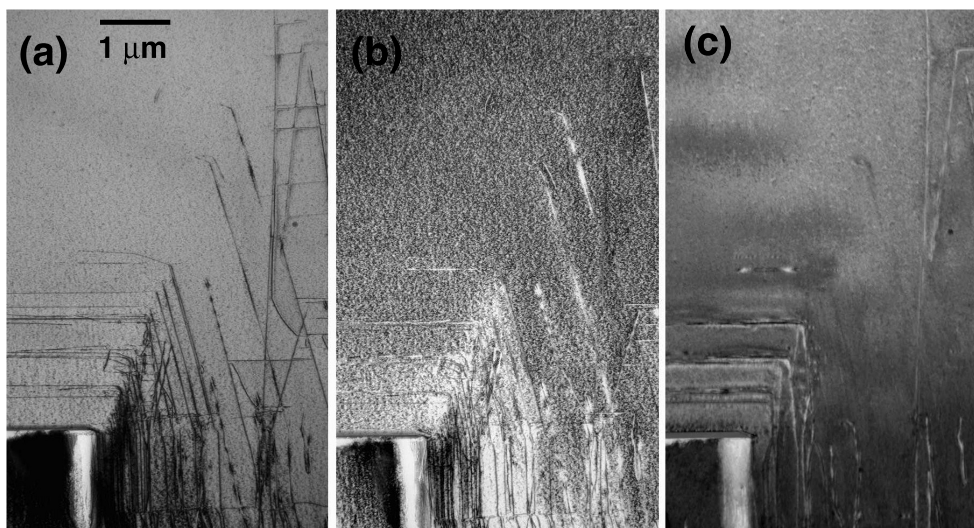

Figure 9. A bright-field image (a) and dark-field images with $g = 11\bar{2}0$ (b) and $g = 0002$ (c) near the mask edge [50].

the mixed dislocations including the component $\boldsymbol{c}$ of the Burgers vector; however, the steps of the FACELO GaN surface form at regular intervals, indicating the excellent surface quality on the atomic scale. Slight irregularities of the steps are seen in the centre of the mask area as indicated by arrows; these come from the line of the dislocations, as seen in figure 8(a).

The optical properties were investigated by means of photoluminescence (PL). Figure 11 shows the PL spectra that were measured using a He–Cd laser (325 nm) from 6.5 K to RT [49]. The luminescence corresponding to free excitons, E_{xA} and E_{xB}, and a bound exciton (D^0, X)

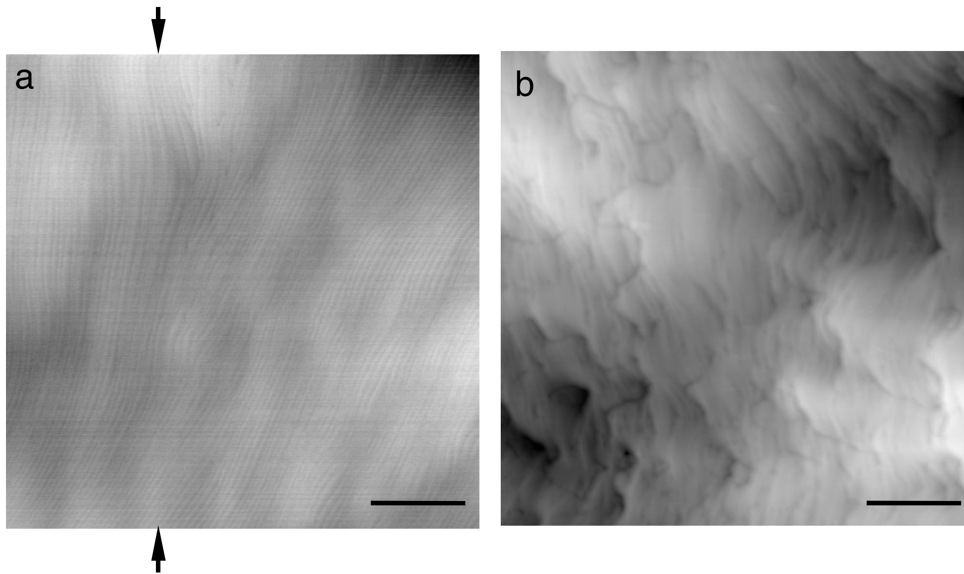

Figure 10. AFM images of (a) as-grown FACELO GaN and (b) as-grown ordinary GaN. The bar indicates 2 μm [49].

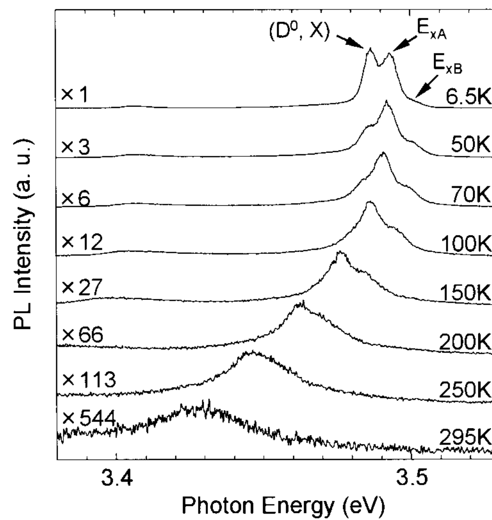

Figure 11. The dependence of PL spectra on temperature [49].

were observed. At 6.5 K, the photon energies of (D^0, X), E_{xA} and E_{xB} are 3.485, 3.492 and 3.500 eV, respectively. The intensities of E_{xA} and E_{xB} are strong at the low temperature of 6.5 K, indicating that the crystal quality of FACELO GaN is fairly good.

3.6. Applications of ELO GaN in optical or electronic devices

Using ELO GaN realizing low dislocation density, the performances of optical or electronic devices, such as light-emitting diodes (LEDs) [51], laser diodes (LDs) [52], field-effect

transistors (FETs) [53] and photodiodes [54, 55], are improved. Nagahama *et al* fabricated an InGaN multi-quantum-well laser diode on low-dislocation-density GaN substrates that were grown on free-standing GaN substrates by ELO [52]. A schematic diagram of the laser structure is shown in figure 12. The threading dislocation density of the GaN layer above the window area surrounding the SiO_2 mask was reduced to 5×10^7 cm^{-2}, and that of the GaN layer above the SiO_2 mask area was reduced to 5×10^7 cm^{-2}. LDs with an output of 30 mW exhibited estimated lifetimes of about 15 000 h under 30 mW operation and 60 °C. Vetury *et al* fabricated an AlGaN/GaN heterostructure field-effect transistor (HFET) on GaN grown by ELO [53]. HFETs on ELO GaN showed substantially lower gate leakage (by up to two orders of magnitude) than HFETs on standard GaN. Parish *et al* and Monroy *et al* fabricated pin and Schottky UV photodetectors, respectively, on ELO GaN [54, 55]. The improved quality of the semiconductor material results in a lower leakage current density, a higher UV/visible contrast, a larger bandwidth and a higher sensitivity in comparison with similar devices on standard GaN on sapphire.

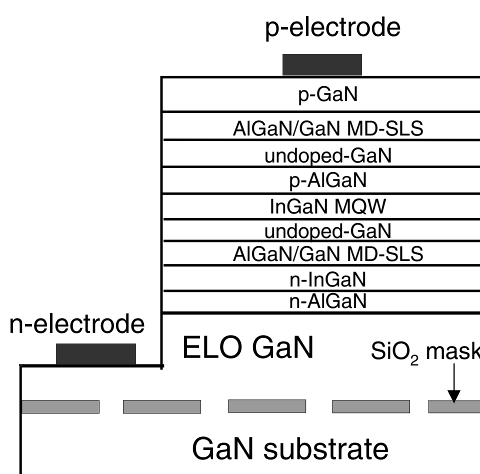

Figure 12. A schematic drawing of InGaN multi-quantum-well laser diodes grown on low-dislocation-density GaN substrates.

4. Summary

The selective area growth and epitaxial lateral overgrowth techniques used in group III nitride epitaxy were reviewed.

Selective-area growth of line-patterned or dot-patterned GaN and AlGaN by MOVPE was carried out on MOVPE-grown GaN(0001)/sapphire substrates using SiO_2 masks. The selectivity was good. Morphological changes occurred on varying the growth conditions. Furthermore, the SAG technique has been developed to apply to cold-cathode emitter tips, low-loss optical waveguides, microprism laser diodes and semiconductor microstructures such as quantum ones.

In order to reduce the dislocation density, various ELO techniques, such as FIELO and PENDEO epitaxy, were developed. FACELO is one of the most effective techniques. The estimated density is of the order of 10^{5-6} cm^{-2} depending on the position of the surface. It was less than that of GaN films on sapphire substrates with low-temperature buffer layers.

Consequently, we can state that the performances of optical or electronic devices, such as light-emitting diodes, laser diodes, field-effect transistors and photodiodes, were improved on using ELO GaN to realize low dislocation density.

Acknowledgments

The author would like to thank Dr H Miyake and Dr A Motogaito for helping to write this article.

References

[1] Kato Y, Kitamura S, Hiramatsu K and Sawaki N 1994 *J. Cryst. Growth* **144** 133
[2] Kitamura S, Hiramatsu K and Sawaki N 1995 *Japan. J. Appl. Phys.* **34** L1184
[3] Nam O H, Bremser M D, Ward B L, Nemanich R J and Davis R F 1997 *Japan. J. Appl. Phys.* **36** L532
[4] Underwood R D, Kapolnek D, Keller B P, Keller S, DenBaars S P and Mishra U K 1997 *Solid State Electron.* **41** 243
[5] Tanaka T, Uchida K, Watanabe A and Minagawa S 1996 *Appl. Phys. Lett.* **68** 976
[6] Akasaka T, Kobayashi Y, Ando S, Kobayashi N and Kumagai M 1998 *J. Cryst. Growth* **189+190** 72
[7] Wang J, Nozaki M, Ishikawa Y, Lachab M, Qhalid Fareed R S, Wang T and Sakai S 1999 *Compound Semiconductors (Inst. Phys. Conf. Ser. 162)* ed H Sakaki *et al* (Bristol: Institute of Physics Publishing) p 829
[8] Li X, Jones A M, Roh S D, Turnbull D A, Reuter E E, Gu S Q, Bishop S G and Coleman J J 1996 *Mater. Res. Soc. Symp. Proc* **395** 943
[9] Kapolnek D, Keller S, Vetury R, Underwood R D, Kozodoy P, DenBaars S P and Mishra U K 1997 *Appl. Phys. Lett.* **71** 1204
[10] Hiramatsu K, Kitamura S and Sawaki N 1996 *Mater. Res. Soc. Symp. Proc.* **395** 267
[11] Underwood R D, Kapolnek D, Keller B P, Keller S, DenBaars S P and Mishra U K 1995 *Proc. Topical Workshop on III–V Nitrides* p 181
[12] Kapolnek D, Underwood R D, Keller B P, Keller S, DenBaars S P and Mishra U K 1997 *J. Cryst. Growth* **170** 340
[13] Beaumont B, Haffouz S and Gibart P 1998 *Appl. Phys. Lett.* **72** 921
[14] Kawaguchi Y, Honda Y, Matsushima H, Yamaguchi M, Hiramatsu K and Sawaki N 1998 *Japan. J. Appl. Phys.* **37** L966
[15] Kawaguchi Y, Honda Y, Yamaguchi M, Hiramatsu K and Sawaki N 1999 *Compound Semiconductors (Inst. Phys. Conf. Ser. 162)* ed H Sakaki *et al* (Bristol: Institute of Physics Publishing) p 687
[16] Matsushima H, Yamaguchi M, Hiramatsu K and Sawaki N 1998 *J. Cryst. Growth* **189+190** 78
[17] Akasaka T, Kobayashi Y, Ando S and Kobayashi N 1997 *Appl. Phys. Lett.* **71** 2196
[18] Kapolnek T D, Keller S, Underwood R D, Kozodoy P, DenBaars S P and Mishra U K 1998 *J. Cryst. Growth* **189+190** 83
[19] Hoffmann A, Siegle J, Kaschner A, Eckey L, Thomsen C, Christen J, Bertram F, Schmidt M, Hiramatsu K, Kitamura S and Sawaki N 1998 *J. Cryst. Growth* **189+190** 630
[20] Tachibana K, Someya T, Ishida S and Arakawa Y 2000 *Appl. Phys. Lett.* **76** 3212
[21] Nishinaga T, Nakano T and Zhang S 1988 *Japan. J. Appl. Phys.* **27** L964
[22] Ujiie Y and Nishinaga T 1989 *Japan. J. Appl. Phys.* **28** L337
[23] Usui A, Sunakawa H, Sakai A and Yamaguchi A 1997 *Japan. J. Appl. Phys.* **36** L899
The first idea was proposed by
Nishinaga T, Nakano T and Zhang S 1988 *Japan. J. Appl. Phys.* **27** L964
[24] Nam O H, Bremser M D, Zheleva T S and Davis R F 1997 *Appl. Phys. Lett.* **71** 2638
[25] Sakai A, Sunakawa H and Usui A 1997 *Appl. Phys. Lett.* **71** 2259
[26] Zheleva T S, Smith S A, Thomson D B, Gehrke T, Linthicum K J, Rajagopal P, Carlson E, Ashmawi W M and Davis R F 1999 *Mater. Res. Soc. Symp. Proc.* **537** G3.38
[27] Kawaguchi Y, Nambu S, Sone H, Shibata T, Matsushima H, Yamaguchi M, Miyake H, Hiramatsu K and Sawaki N 1998 *Japan. J. Appl. Phys.* **37** L845
[28] Sone H, Nambu S, Kawaguchi Y, Yamaguchi M, Miyake H, Hiramatsu K, Iyechika Y, Maeda T and Sawaki N 1999 *Japan. J. Appl. Phys.* **38** L356
[29] Kidoguchi I, Ishibashi A, Sugahara G and Ban Y 2000 *Appl. Phys. Lett.* **76** 3768

[30] Kidoguchi I, Ishibashi A, Sugahara G, Tsujimura A and Ban Y 2000 *Japan. J. Appl. Phys.* **39** L453
[31] Detchprohm T, Yano M, Sano S, Nakamura R, Mochiduki S, Nakamura T, Amano H and Akasaki I 2001 *Japan. J. Appl. Phys.* **40** L16
[32] Zhang X, Li R R, Dapkus P D and Rich D H 2000 *Appl. Phys. Lett.* **77** 2213
[33] Hiramatsu K, Nishiyama K, Motogaito A, Miyake H, Iyechika Y and Maeda T 1999 *Phys. Status Solidi* a **176** 535
[34] Beaumont B, Bousquet V, Vennéguès P, Vaille M, Bouillé A, Gibart P, Dassonneville S, Amokrane A and Sieber B 1999 *Phys. Status Solidi* a **176** 567
[35] Nam O H, Zheleva T S, Bremser M D, Thomson D B and Davis R F, 1998 *Mater. Res. Soc. Symp. Proc.* **482** 301
[36] Park J, Grudowski P A, Eitting C J and Dupuis R D 1998 *Appl. Phys. Lett.* **73** 333
[37] Coltrin M E, William C C, Bartram M E, Han J, Missert N, Crawford M H and Baca A G 1999 *Mater. Res. Soc. Symp. Proc.* **537** G6.9
[38] Zhang R, Zhang L, Hansen D M, Boleslawski M P, Chen K L, Lu D Q, Shen B, Zheng Y D and Kuech T F 1999 *Mater. Res. Soc. Symp. Proc.* **537** G4.7
[39] Marchand H, Ibbetson J P, Fini P T, Wu X H, Keller S, DenBaars S P, Speck J S and Mishra U K 1999 *Mater. Res. Soc. Symp. Proc.* 537 G4.5
[40] Miyake H, Motogaito A and Hiramatsu K 1999 *Japan. J. Appl. Phys.* **38** L1000
[41] Tadatomo K, Ohuchi Y, Okagawa H, Itoh H, Miyake H and Hiramatsu K 1999 *Mater. Res. Soc. Symp. Proc.* **537** G3.1
[42] Kawaguchi Y, Nambu S, Yamaguchi M, Sawaki N, Miyake H, Hiramatsu K, Tsukamoto K, Kuwano N and Oki K 1999 *Phys. Status Solidi* a **176** 561
[43] Beaumont B, Haffouz S and Gibart P 1998 *Appl. Phys. Lett.* **72** 921
[44] Kung P, Walker D, Hamilton M, Diaz J and Razeghi M 1999 *Appl. Phys. Lett.* **74** 570
[45] Kawaguchi Y, Honda Y, Yamaguchi M, Sawaki N and Hiramatsu K 1999 *Phys. Status Solidi* a **176** 553
[46] Hiramatsu K, Kawaguchi Y, Shimizu M, Sawaki N, Zheleva T S, Davis R F, Tsuda H, Taki W, Kuwano N and Oki K 2000 *MRS Internet J. Nitride Semicond.* **Res.2** 6
[47] Kawaguchi Y, Shimizu M, Yamaguchi M, Hiramatsu K, Sawaki N, Taki W, Tsuda H, Kuwano N, Oki K, Zheleva T and Davis R F 1998 *J. Cryst. Growth* **189+190** 24
[48] Kagawa K, Horibuchi K, Kuwano N, Oki K and Hiramatsu K 2000 *Proc. Int. Workshop on Nitride Semiconductors (IPAP Conf. Ser. 1)* (Tokyo: The Institute of Pure and Applied Physics) p 471
[49] Hiramatsu K, Nishiyama K, Mizutani H, Narukawa M, Motogaito A, Miyake H, Iyechika Y and Maeda T 2000 *J. Cryst. Growth* **221** 316
[50] Honda Y, Iyechika Y, Maeda T, Miyake H and Hiramatsu K 2001 *Japan. J. Appl. Phys.* **40** L309
[51] Nakamura S 2000 *IEICE Trans. Electron.* **E83-C** 529
[52] Nagahama S, Iwasa N, Senoh M, Matsushita T, Sugimoto Y, Kiyoku H, Kozai T, Sano M, Matsumura H, Umemoto H, Chocho K and Mukai T 2000 *Japan. J. Appl. Phys.* **39** L647
[53] Vetury R, Marchand H, Parish G, Fini P T, Ibbetson J P, Keller S, Speck J S, DenBaars S P and Mishra U K 1999 *Compound Semiconductors (Inst. Phys. Conf. Ser. 162)* ed H Sakaki *et al* (Bristol: Institute of Physics Publishing) p 177
[54] Parish G, Keller S, Kozodoy P, Ibbetson J P, Marchand H, Fini P T, Fleischer S B, DenBaars S P and Mishra U K 1999 *Appl. Phys. Lett.* **75** 247
[55] Monroy E, Calle F, Munoz E, Beaumont B, Omnès F and Gibart P 1999 *Phys. Status Solidi* a **175** 141